Experimental evidence for spin diffusion in the quasi-two-dimensional Heisenberg paramagnet $(C_2H_5NH_3)_2MnCl_4$

H. Benner
Institut für Festkörperphysik, Technische Hochschule Darmstadt, D-6100 Darmstadt, Federal Republic of Germany
(Received 12 December 1977)

High-temperature spin dynamics in the quasi-two-dimensional Heisenberg system ethylammonium-manganesechloride have been investigated by EPR with very high sensitivity. Two different experimental methods are presented which can be used to analyze the resonances of the respective memory spectrum occurring at the Larmor frequency ω_0 and at $2\omega_0$. Around ω_0 the memory spectrum is obtained from the absorption and dispersion part of the transversal susceptibility. The resonance behavior at $2\omega_0$ can be obtained directly from a satellite structure at half EPR field which has been observed in the transversal and in the longitudinal susceptibility. For both resonances a logarithmic shape is determined which—as theory predicts—is due to spin diffusion. There is some experimental evidence for a decoupling of the 4-spin correlation function for long times. The spin-diffusion constant is evaluated to be $D/a^2 = 13 \pm 2$ K.

I. INTRODUCTION

During the last few years high-temperature spin dynamics of one-dimensional (1D) or two-dimensional (2D) Heisenberg magnets have been widely investigated, theoretically as well as experimentally. The influence of dimensionality occurs most pronounced in those physical properties which are connected to $q \approx 0$ modes; magnetic resonance, therefore, has proven to be a powerful tool in its investigation. In the limit $q = 0$ dynamics are governed by long-wave fluctuations whose long-time behavior is subject to a diffusion law. With EPR, for instance, these diffusive modes have been shown to lead to considerable deviations from the Lorentzian shape, well known from the exchange-narrowed lines of normal three-dimensional systems, and to a characteristic linewidth anisotropy due to secular contributions of the dipolar interaction.[1-4] In spite of quite a number of experimental results, these effects were discussed for years in a more qualitative way, and quantitative proofs of spin diffusion have only been reported very recently on the 1D system TMMC $[(CH_3)_4NMnCl_3]$. Analyzing the EPR linewidth and dynamical shift at the magic angle Lagendijk *et al.*[5] found for both a frequency dependence of $\omega^{-1/2}$ which is characteristic for 1D spin diffusion. The same frequency dependence was obtained by Boucher *et al.*[6] by NMR from T_1 measurements for the spectral density of the electronic two-spin correlation function. For 2D systems such an experimental proof of spin diffusion has not been furnished yet.

The question is how, in principle, to establish such a proof by the investigation of transversal susceptibility. If there are any long-time contributions to the underlying memory function $\gamma^+(t)$ they will cause a frequency dependence in its spectral density $\gamma^+(\omega)$. As is long known from theory, a resonance peak of $\gamma^+(\omega)$ occurs not only at the Larmor frequency ω_0 but—depending on orientation—additional sidebands are expected at $-\omega_0$, 0, and $2\omega_0$. The latter one has been observed in 1D systems just recently.[7] This is illustrated by Fig. 1(b). The shape of these resonance peaks depends in characteristic manner on the long-time behavior of the memory function. That means, if spin diffusion takes place we shall find a resonance behavior approximately like $[\omega-(m+1)\omega_0]^{-1/2}$ for the 1D case and like $-\ln[\omega-(m+1)\omega_0]$ for the 2D case, m being integer from -2 to $+1$. For example, when looking at the magic-angle EPR linewidth of a 1D system the "secular" resonance ($m=0$) is removed by orientation and one samples the contributions from the wings of all "nonsecular" ($m \neq 0$) sidebands at the frequency $\omega = \omega_0$ which behave like $\omega^{-1/2}$. For a 2D system, however, this technique is not expected to be effective as the linewidth is mainly due to short-time decay of the memory function, and linewidth contributions from spin diffusion are of less importance. In this work another method shall be tried. The resonance behavior of the secular and of the $m=1$ nonsecular peak shall be analyzed at their own resonance frequency. For the secular peak it can be done by a very sensitive line-shape analysis of the normal EPR line covering both absorption and dispersion, and for the $m=1$ nonsecular peak the desired frequency dependence is directly derived from a new type of

 ©1978 The American Physical Society

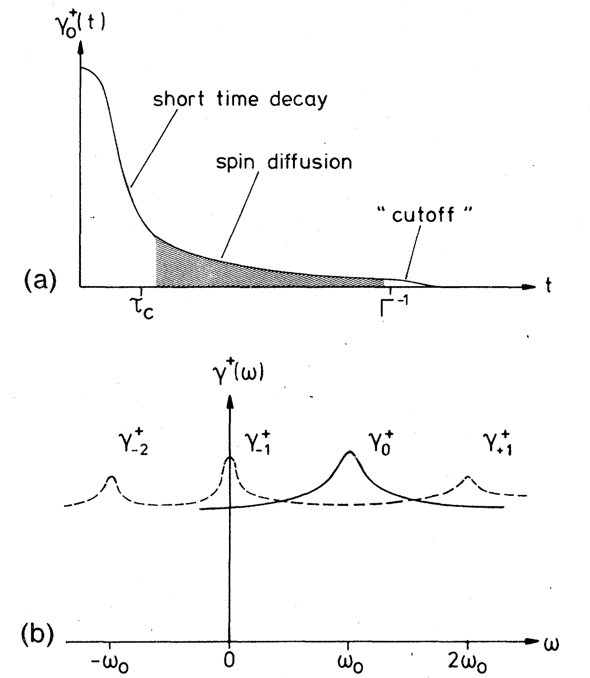

FIG. 1. (a) Typical curve of the memory function in a 2D system (secular contribution only). $\tau_c = \hbar/J$, where J is the exchange integral. Γ is given by the EPR linewidth. (b) Resonance peaks in the memory spectrum (schematically); solid line: only secular contribution ($\theta=0°$; θ is the angle between c axis and magnetic field); dashed line: only nonsecular contributions ($\theta=54°$).

satellite line at half resonance field, for the first time observed just recently.[7]

In Sec. II the theory of EPR on low-dimensional systems shall be presented as far as necessary for the interpretation of our experimental results. Based upon that a simple expression is derived which accounts for the observed qualities of the half-field satellite in a rather satisfactory way. For a more complete survey the reader has to refer to the literature.[4,6–8] Experimental details are given in Sec. III which is followed by a discussion of the results.

II. THEORY

The Hamiltonian of the system to be discussed shall consist of a Zeeman term H_Z, a dipolar interaction H_D, and a dominating Heisenberg exchange coupling H_{ex}

$$H = H_Z + H_D + H_{\text{ex}} \ . \tag{1}$$

The $q=0$ transversal dynamic susceptibility χ_+ we are interested in can be described by the spectral density of the memory function—which shall be called in short the memory spectrum $\gamma^+(\omega,H)$—according to

$$\chi_+(\omega,H) = \chi_0^+\left[1 - \frac{i\omega}{i(\omega-\omega_0)+\gamma^+(\omega,H)}\right] \ , \tag{2}$$

where ω stands for the microwave frequency, $\omega_0 = g\mu_B\hbar^{-1}H$ for the Larmor frequency, χ_0^+ for the static transversal susceptibility, and $\gamma^+(\omega,H)$ for the half-side Fourier transform of the memory function which under the Hamiltonian (1) turns out to be a correlation function of fluctuations in dipolar field. The EPR signal is normally related to the imaginary part of $\chi_+(\omega,H)$ via

$$\chi_+''(\omega,H) \propto \frac{\mathrm{Re}[\gamma^+(\omega,H)]}{(\omega-\omega_0)^2 + \{\mathrm{Re}[\gamma^+(\omega,H)]\}^2} \ , \tag{3}$$

where, for simplification, the imaginary part of $\gamma^+(\omega,H)$ has been neglected, as a discussion of the dynamical shift is not intended. In the following $\mathrm{Re}[\gamma^+(\omega,H)]$ shall be denoted by $\gamma^+(\omega,H)$.

Trying to explain EPR spectra requires knowledge of the frequency and field dependence of γ^+ which can, at least in approximation, be derived from a microscopic theory. Taking into consideration secular as well as nonsecular contributions from the dipolar interaction, the memory function is given by

$$\gamma^+(t,H) = \frac{\omega_D^2}{k_B T N \chi_0^+} \sum_q \sum_{m=-2}^{1} |F_q^m|^2 \Sigma_q^\alpha(t)\,\Sigma_q^\beta(t) \ ,$$
$$\alpha+\beta = m+1 \ . \tag{4}$$

Here, the indices α and β refer to spherical coordinates and can have the values 0 and ± 1. $\omega_D = g^2\mu_B^2 a^{-3}$ is the dipolar coupling constant for a lattice with the nearest-neighbor distance a, k_B the Boltzmann constant, and T the temperature. The F_q^m are geometrical coefficients resulting from a summation of dipolar contributions over all sites of a square lattice. For small q values they depend on angle θ—which indicates the difference between the c axis and direction of magnetic field—as follows[3]

$$|F_0^0|^2 \propto (3\cos^2\theta - 1)^2 \ , \tag{5a}$$

$$|F_0^{\pm 1}|^2 \propto \sin^2\theta\cos^2\theta \ , \tag{5b}$$

$$|F_0^{\pm 2}|^2 \propto \sin^4\theta \ . \tag{5c}$$

The $\Sigma_q^\alpha(t)$, finally, denote two-spin correlation functions which can be described for a 2D system in good approximation by

$$\Sigma_q^\alpha(t) = k_B T \chi_q^\alpha e^{-Dq^2 t - \Gamma^\alpha t + i\alpha\omega_0 t} \ , \tag{6}$$

where χ_q^α represents the static wave-vector dependent susceptibility. For sufficiently large q the decay of $\Sigma_q^\alpha(t)$ is dominated by term Dq^2, that means damping is due to isotropic exchange interaction and the modes behave diffusively. In the limit $q=0$, however, anisotropic dipolar interaction provides for the nonvanishing of damping by a q-independent contribution Γ^α.

As the two-spin correlation function is connected with the dynamical susceptibility by Fourier transformation, Γ^+ has—by definition—to be identified with $\gamma^+(\omega=\omega_0)$ and is directly given by the EPR linewidth. Thus, Eq. (4) may be regarded as a self consistent equation for the two-spin damping constant in the limit $q=0$ for a given diffusion constant D. It is important to mention that Eq. (4) has been deduced within the bounds of the independent-mode approximation, that means a decoupling of four-spin correlation functions originally occurring in the expression of $\gamma^+(t,H)$ according to the scheme

$$\begin{aligned}\langle S_q^\alpha(t) S_{-q}^\beta(t) S_{q'}^{-\alpha'} S_{-q'}^{-\beta'}\rangle \\ \approx [\delta_{\alpha\alpha'}\delta_{\beta\beta'}(q+q') + \delta_{\alpha\beta'}\delta_{\beta\alpha'}\delta(q-q')] \\ \times \langle S_q^\alpha(t) S_{-q}^{-\alpha}\rangle \langle S_q^\beta(t) S_{-q}^{-\beta}\rangle \ , \qquad (7)\end{aligned}$$

where δ stands for both the Kronecker symbol and the Dirac δ function, and the brackets denote the high-temperature statistical average. Although this procedure is customary when dealing with higher correlation functions, it cannot be justified rigorously, and some doubts have arisen already whether it could be responsible for discrepancies between calculated and measured linewidths in other systems.

Reiter and Boucher[8] have solved Eq. (4) for the special orientation $\vec{H} \parallel \vec{c}$ where all but the $m=0$ term disappear. Their result shall be used in Sec. IV to analyze the field dependence of $\gamma^+(\omega,H)$ and to evaluate the diffusion constant. As illustrated by Fig. 1(b), they obtain for $\gamma^+(\omega,H)$ a weak logarithmic resonance at ω_0 which coincides with the much stronger resonance behavior of the denominator of $\chi_+(\omega,H)$ in Eq. (3) and will cause only slight deviation from a Lorentzian in the EPR line shape.

If the magnetic field is no longer supposed to be parallel to the c axis, that means perpendicular to the layers, additional nonsecular contributions have to be taken into account. In that case, however, a self-consistent treatment would be far more complicated. If there is no intention to investigate the influence of nonsecular contributions on the main line in detail but only to discuss the properties of half-field satellites in a 2D system, a simpler method which we have developed can be used as follows. If confining to the $m=1$ term, responsible for the resonance at $2\omega_0$, Eq. (4) can be evaluated by introducing $\Gamma^+=\Gamma^+(\theta)$ phenomenologically. This works because Γ^+ is the only damping constant in the expression for $\gamma_{m=1}^+(t,H)$ and is directly obtained from the width of the main line. Substitution of Eq. (6) in (4) and Fourier transformation yield

$$\gamma_{m=1}^+(\omega,H) = \frac{3}{8\pi} S(S+1)\omega_D^2 |F_{q=0}^{m=1}(\theta)|^2 a^2 D^{-1} \times \mathrm{Re}\left[\ln\left(1+\frac{8\pi D a^{-2}}{2\Gamma^+(\theta)+i(\omega-2\omega_0)}\right)\right] \ , \qquad (8)$$

where the q dependence of the geometrical coefficient has been neglected, the q summation has been replaced by an integration over a circular Brillouin zone, and the χ_q have been taken in the high-temperature limit. The validity of such simplifications has already been discussed in detail.[4,7,8] It is convenient to introduce the dimensionless parameter

$$\epsilon = \frac{3S(S+1)\omega_D^2 a^2}{32\pi D \Gamma^+(\theta=0)} |F_{q=0}^{m=0}(\theta=0)|^2 \ , \qquad (9)$$

which also appears in the result of Reiter and Boucher. By slight simplification of the logarithmic expression for the condition $\Gamma^+ << 8\pi D a^{-2}$, which will turn out to be valid, one obtains

$$\gamma_{m=1}^+(\omega,H) = \Gamma\epsilon \sin^2\theta\cos^2\theta \times \left\{\mathrm{const} - \ln\left[1+\left(\frac{\omega-2\omega_0}{2\Gamma^+(\theta)}\right)^2\right]^{1/2}\right\} \ . \qquad (10)$$

It can be shown that the constant is in the order of ϵ^{-1}, and Γ denotes $\Gamma^+(\theta=0)$. The $m\neq 1$ terms, also present in the memory spectrum, may be considered as being field or frequency independent in the respective region. Thus, at $\omega\approx 2\omega_0$ the memory spectrum consists of a constant part $A(\theta)$ describing the Lorentzian wings of the main line and of a frequency dependent part showing resonance behavior which will lead to an additional satellite in the EPR spectrum at half-resonance field

$$\chi_+''(\omega\approx 2\omega_0) = \left\{A(\theta) - \frac{\Gamma\epsilon}{2}\sin^2\theta\cos^2\theta \times \ln\left[1+\left(\frac{\omega-2\omega_0}{2\Gamma^+(\theta)}\right)^2\right]\right\}(\omega-\omega_0)^{-2} . \qquad (11)$$

It should be emphasized that—contrary to the main line—this satellite is scarcely influenced by the frequency dependence of the denominator of Eq. (3) but represents directly the $m=1$ resonance of the memory spectrum. The resonance should be observable whenever the long-time behavior of the memory function contributes noticeably to the linewidth or influences the shape of the main line.

Therefore, according to Eq. (11) the satellite is expected to show the following characteristic properties: (a) a strong intensity dependence on orientation, proportional to $\sin^2\theta\cos^2\theta$, (b) a line shape described by the logarithmic expression of Eq. (11) which differs significantly from the common Lorentzian, and (c) a linewidth $\Gamma^+(\theta)$ which coincides with the width of the main line. The second and especially the third property have been derived as a direct consequence of the decoupling procedure mentioned above. The experimental confirmation, therefore, would be of considerable theoretical interest.

The proof can be obtained not only from the transversal but also from the longitudinal susceptibility where the half-field satellite is expected to occur, too. The calculation turns out to be rather similar to the one above and shall not be mentioned here in detail. The result for the half-field resonance differs from Eq. (11) only by a factor of ω^{-2} instead of $(\omega-\omega_0)^{-2}$, and by the angular intensity dependence which behaves like $\sin^4\theta$ instead of $\sin^2\theta\cos^2\theta$. Linewidth and line shape, however, are expected to be exactly the same as in the transversal case and should, therefore, be part of the following investigation.

III. EXPERIMENTAL

Ethylammonium-manganesechloride $[(C_2H_5NH_3)_2MnCl_4]$ is well known as a quasi-2D layer structure.[9] It consists of nearly quadratic layers of manganese ions with strong isotropic antiferromagnetic exchange interaction within the plane but—due to separation by organic ethyl and by ammonium groups—with an extremely small interaction between neighboring planes which has been estimated to be less than 10^{-9} of the in-plane interaction.[10] Three-dimensional antiferromagnetic order occurs below 43 K, it can, therefore, be assumed that the system shows high-temperature behavior already at room temperature.

Single crystals were grown from aqueous solution as already reported.[11] The EPR experiments were performed at room temperature with commercial Varian spectrometers of type E9 in X band and of type V 4502 in Q band. The aim was to study absorption and dispersion far out in the wings of the main line in order to get information on the memory spectrum which requires a very good signal-to-noise ratio. The EPR spectra, however, should not be affected by cavity overloading, and base-line drifts had to be carefully avoided. This was achieved by combining the normal lock-in technique with signal averaging in a 1024 channel analyzer (Fabri-Tek 1072). Scans of the absorption and of the dispersion derivative were sampled alternately in order to minimize errors in amplitude by these "quasisimultaneous" measurements of both spectra. The data were transferred to a computer where $\chi'(H)$ and $\chi''(H)$ were obtained by integration in connection with a very sensitive base-line fit and evaluated as discussed below. Details of this procedure shall be published elsewhere. Half-field satellites of $(C_2H_5NH_3)_2MnCl_4$ have been observed in X and Q band in the longitudinal as well as in the transversal susceptibility. The samples used in these experiments were much larger than in the experiment above, for the maximum satellite line intensity turned out to be less than 10^{-5} of the main-line intensity. With a sample size of $6\times6\times1.5\text{mm}^3$ in X band and $2\times2\times1$ mm^3 in Q band, the signal-to-noise ratio was sufficient to allow a line-shape analysis. The X band measurements of transversal absorption were performed in a Varian E 231 rectangular cavity. As the main-line wings were already larger in intensity at half-resonance field than the satellite, they had to be subtracted very carefully in order to get the correct satellite linewidth and shape. For measurement of the longitudinal absorption the samples were put on the bottom of a home-built rectangular cavity. The magnetic field was precisely oriented parallel to the microwave field at sample position by minimizing the main-line intensity at normal resonance field. The requirement of rotating the sample with respect to the magnetic field will diminish the homogeneity of the microwave field if larger samples are used because the platelets have to be moved edgewise. Therefore, a small piece, size $6\times1.5\times1.5$ mm^3, was cut off a platelet and fixed to the bottom of the cavity with the c axis parallel to it. Rotating the bottom, the angle θ could be varied without affecting the microwave field too much. Due to smaller sample size, the signal-to-noise ratio of the longitudinal spectra was worse by one magnitude, except for the orientation $\theta=90°$ where a larger platelet could be put flat on the bottom. Analyzing the half-field satellite in the longitudinal configuration has the advantage that the main line theoretically should not exist which means, in practice, that its intensity is strongly reduced. Q-band measurements on the satellites were accomplished only for the transversal case with a home-built cylindric cavity. Though the relative satellite intensity should decrease like ω^{-2}, its structure appeared even more pronounced due to larger separation from the main-line resonance which, at half-resonance field, causes its wings in the derivative spectrum to be reduced like ω^{-3}.

IV. DISCUSSION OF THE RESULTS

At first, we want to deal with the resonance behavior of the memory spectrum at $\omega=\omega_0$ which is due to the long-time behavior of the secular contribution of the dipolar interaction. From Eq. (2) the relation

$$\gamma^+(\omega,H)=\frac{\chi''(\omega,H)}{[\chi'(\omega,H)]^2+[\chi''(\omega,H)]^2} \tag{12}$$

is derived which is appropriate for evaluation of the experimental data. $\chi'(\omega,H)$ stands only for the dynamical part of dispersion without the $\omega=0$ contribution. Figure 2 represents the field dependence of $\gamma^+(\omega,H)$ for $\theta=0$ as obtained from the integrated Q-band absorption and dispersion spectra. Although the experimental error—mainly connected with the uncertainty of the base-line fit—is rather large in the outer parts of the wings, the shape of the spectrum looks typical for a layered paramagnet: there is a large constant amount corresponding to a rapid short time decay of $\gamma^+(t)$ and responsible for the almost Lorentzian character of the EPR main line, and a small peak on

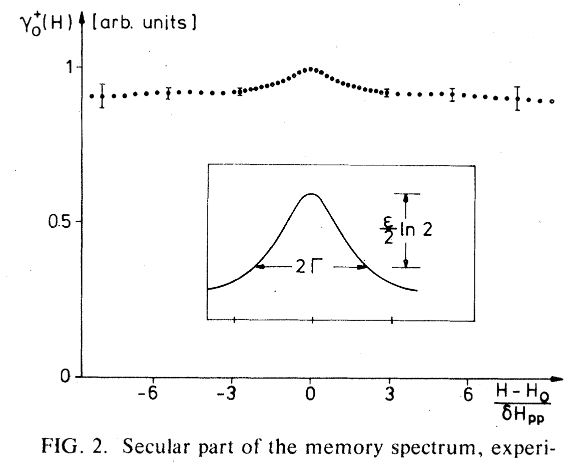

FIG. 2. Secular part of the memory spectrum, experimentally obtained from the absorption and dispersion lineshape at $\theta=0$. The insert shows the resonance peak enlarged by a factor of 4, illustrating the connection between Γ and ϵ. δH_{pp} refers to the main linewidth at $\theta=0$.

its center that refers to spin diffusion. In Fig. 3 a shape analysis of this peak is shown. For the orientation $\vec{H}\parallel\vec{c}$, chosen in experiment, all but the secular part of the memory spectrum vanish, so that the result of Reiter and Boucher[8]

$$\gamma^+(\omega,H)=\Gamma-\tfrac{1}{2}\Gamma\epsilon\ln\left[1+\left(\frac{H-H_0}{\Gamma\hbar/g\mu_B}\right)^2\right] \tag{13}$$

can be used for interpretation. For the special plot, as chosen in Fig. 3, a straight line is expected from Eq. (13). Even though such a representation is not overly sensitive, the experimental data are in quite good agreement with the theoretically predicted logarithmic resonance behavior, and provide a first quantitative proof for spin diffusion.

In the following, it will be shown how the investigation of half-field satellites supplements this information. The most striking feature of this new type of resonance is the strong angular dependence of its intensity which has its maximum at $\theta=90°$ in the longitudinal case, and at $\theta=50°$ in the transversal one, as is roughly expected from the angular dependence of the geometrical coefficients. In experiment, however, the derivative of χ'' with respect to the field is recorded, therefore the intensities given by Eq. (5b) have to be weighted with the reciprocal linewidth $(\delta H_{pp})^{-1}$ when directly compared to the maximum intensity I'_{max} of the derivative, which is done in Fig. 4 for the transversal X-band spectra. Due to linewidth anisotropy, the theoretical curve of $I'(\theta)$ no longer takes a $\sin^2\theta\cos^2\theta$ course but becomes asymmetric and fits the experimental results rather well.

A very important point of this study is to find out whether the satellite lineshape can also be described by a logarithmic resonance, for this would be a direct experimental proof of spin diffusion in a layered system which is even more sensitive than the representation in Fig. 3. Equation (11) yields the absorption derivative with respect to the field as

$$\frac{d}{dH}\chi_+''(H\approx H_0/2)$$
$$\propto\frac{H-H_0/2}{[(H-H_0/2)^2+(\Gamma^+)^2](H-H_0)^2}\ , \tag{14a}$$

for the transversal and

$$\frac{d}{dH}\chi_0''(H\approx H_0/2)\propto\frac{H-H_0/2}{(H-H_0/2)^2+(\Gamma^+)^2}\ , \tag{14b}$$

for the longitudinal case.

Plotting $(H-H_0/2)I'(H)$ vs $(H-H_0/2)^2$, where $I'(H)$ denotes only the satellite intensity, a straight line is expected according to theory. In both, the longitu-

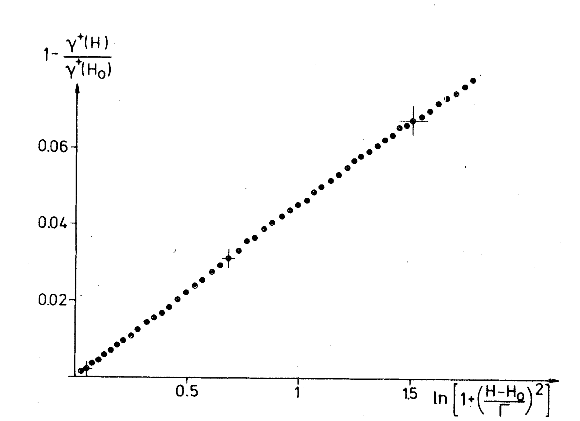

FIG. 3. Shape analysis of the ω_0 resonance peak. Γ has been directly determined as the half maximum width of the (integrated) absorption line at $\theta=0$.

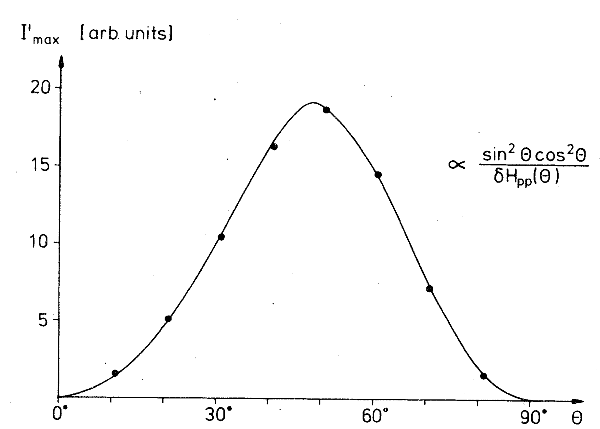

FIG. 4. Angular dependence of the satellite peak-to-peak height of transversal absorption in X band. The solid line indicates the theoretical curve where the data of Fig. 6 have been used for $\delta H_{pp}(\theta)$.

dinal and the transversal case, excellent agreement exists with the experimental data of Fig. 5. Due to factor $(H-H_0)^{-2}$, a correction of $I'(H)$ had to be applied in the latter case. It amounts up to 20% for the field region in question. For comparison, in the same diagram the shape of the main line has been plotted at $\theta=50°$ which looks exactly Lorentzian. Thus, not only the existence of half-field satellites supports present ideas on the dynamics of low dimensional systems but, moreover, the satellite line shape yields a direct quantitative proof of spin diffusion in 2D systems.

With the help of Eqs. (11) and (13) we are now able to evaluate the spin-diffusion constant in different ways. The $m=0$ resonance of the memory spectrum yields parameter ϵ directly as the slope of the straight line in Fig. 3 which results in

$$\epsilon=0.09\pm0.01 \ .$$

Taking Γ from experiment where the EPR linewidth has been assumed to be entirely due to dipolar interaction, evaluating ω_D from the lattice parameter $a'=\sqrt{2}a=7.28$ Å (Ref. 12), and calculating $F_{q=0}^{m=0}(\theta=0)$ by summation of all dipolar contributions from a square lattice, the diffusion constant can be evaluated via Eq. (9) to be

$$D/a^2=15\pm3 \text{ K} \ .$$

To test this experimental result, Eq. (27) of Ref. 8 can be used. There, within the self-consistent treatment, a relation for ϵ has been deduced which requires only the knowledge of Γ, ω_D, and $F_{q=0}^{m=0}(\theta=0)$. Thus, with the above used values the equation can be solved by iteration which yields $\epsilon=0.096$. From the accordance of both results a line-shape analysis seems to be appropriate for the evaluation of the diffusion constant, the expenses, however, are rather large.

An alternative method, dealing with the $m=1$ resonance, is the comparison of satellite and main line intensity. From Eq. (11) the maximum intensity of the satellite derivative spectrum is expressed by

$$I'^{\,\text{sat}}_{\text{max}}(\theta)=2\chi_0\sin^2\theta\cos^2\theta\Gamma\epsilon/\Gamma^+(\theta)\omega \ . \qquad (15)$$

The main line can be well approximated by a Lorentzian for every orientation which leads to

$$I'^{\,\text{main}}_{\text{max}}(\theta)=\frac{3\sqrt{3}}{8}\chi_0\omega[\Gamma^+(\theta)]^{-2} \ . \qquad (16)$$

Thus, parameter ϵ is obtainable from the intensity ratio of satellite and main line derivative according to

$$\epsilon=\frac{3\sqrt{3}I'^{\,\text{sat}}_{\text{max}}(\theta)\omega^2}{16I'^{\,\text{main}}_{\text{max}}(\theta)\Gamma\Gamma^+(\theta)\sin^2\theta\cos^2\theta} \ , \qquad (17)$$

which provides a rather easy way to determine the diffusion constant directly from the EPR spectrum.

For $\theta=50°$ experiment yields an intensity ratio of $(5.0\pm.1)\times10^{-6}$. Applying the value of Fig. 6 to $\Gamma^+(\theta)$ results in $\epsilon=0.104\pm0.012$ which determines the diffusion constant value as

$$D=13\pm2 \text{ K} \ .$$

Provided that apparative effects, like cavity overloading, have been carefully avoided, the second method looks not only simpler but even more sensitive. For $(C_2H_5NH_3)_2MnCl_4$ the exchange integral J is not exactly known yet. From comparison with the isomorphic methyl compound it can be estimated to be 5 K.[9] Thus, the experimentally obtained diffusion constant turns out to be about $0.9J[S(S+1)]^{1/2}$, which is in very good agreement with the theoretical result of Morita,[13] to our knowledge the only one given so far for a square lattice and $S=\frac{5}{2}$.

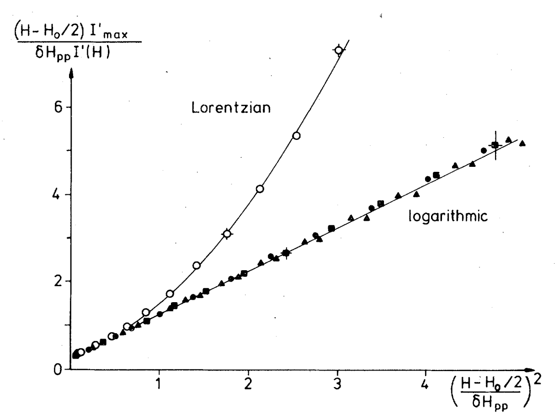

FIG. 5. Shape analysis of the satellite line. ▲, X-band, transversal, $\theta=50°$; ■, X-band, longitudinal, $\theta=90°$; ●, Q-band, transversal, $\theta=50°$. For comparison, the main line shape has also been plotted (○) for the last case.

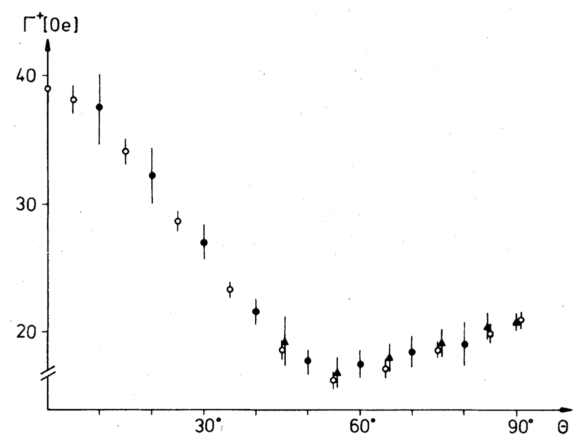

FIG. 6. Angular dependence of Γ^+ in X band in field units. The open circles have been derived from the main line via $\Gamma^+=\sqrt{3}\delta H_{pp}/2$, the full marks from the satellite via $\Gamma^+=\delta H_{pp}/2$ (● transversal, ▲ longitudinal).

Finally, the question shall be discussed whether these experiments can serve to confirm the decoupling procedure mentioned above. As a consequence of the foregoing line-shape analysis it is easily shown that the characteristic width $\Gamma^+(\theta)$ of the satellite is given in field units by exactly half the peak-to-peak linewidth of its derivative. As a direct result of decoupling, this width $\Gamma^+(\theta)$ should coincide with the damping constant of the respective two-spin correlation function in the limit $q=0$ to be obtained from the EPR main-line half-width. This way, two independent measurements of $\Gamma^+(\theta)$ are available. In Fig. 6 the main line half-width is compared to both, the transversal and the longitudinal satellite width. There is not only a complete qualitative agreement but—within the limits of experimental error—also a quantitative one. Thus, from an experimental point of view, it can be said that in a 2D system the decoupling procedure seems to be correct, at least for the long-time behavior of the memory function.

V. SUMMARY AND CONCLUSIONS

Two different experimental methods have been presented as how to analyze by EPR the influence of spin diffusion on high-temperature dynamics in a 2D system. The first one referred to the secular contribution of dipolar interaction to the memory spectrum. From the absorption and dispersion lineshape a distinct resonance peak in the memory spectrum could be obtained at $\omega=\omega_0$. The second method made use of a new type of half-field resonance which is due to the $m=1$ nonsecular contribution and was shown to exhibit directly the properties of the memory spectrum at $\omega=2\omega_0$. The theoretically predicted logarithmic shape has been proven by experiment for both peaks, which may be taken as a first quantitative confirmation of spin diffusion in a 2D system. A comparison of the width of satellite and main line seems to support simple decoupling of the four-spin correlation function, at least for those times when its decay is subject to spin diffusion. In this connection, it would be very interesting to compare the quantitative result of the spin diffusion constant, derived from the memory spectrum, with the value directly obtained from the diffusion behavior of the two-spin correlation function as, for instance, can be measured by NMR. However, such data are not available yet.

ACKNOWLEDGMENTS

The author would like to thank Professor Dr. B. Elschner for his support of this investigation. The first experimental method (absorption/dispersion line-shape analysis) has been suggested by Dr. J. P. Boucher. Discussions with Dr. W. Finger were very useful. The help of A. Maiazza and C. Lauer in sample preparation and computation is gratefully acknowledged.

---

*Project of "Sonderforschungsbereich Festkörperspektroskopie Darmstadt/Frankfurt," financed by special funds of the Deutsche Forschungsgemeinschaft.

[1]R. E. Dietz, F. R. Merrit, R. Dingle, D. Hone, B. Silbernagel, and P. M. Richards, Phys. Rev. Lett. 26, 1186 (1971).

[2]M. J. Hennessy, C. D. McElwee, and P. M. Richards, Phys. Rev. B 7, 930 (1973).

[3]P. M. Richards and M. B. Salamon, Phys. Rev. B 9, 32 (1974).

[4]P. M. Richards, in *Local Properties at Phase Transitions, Proceedings of the International School of Physics "Enrico Fermi"* (North-Holland, Amsterdam, 1976), p. 539.

[5]A. Lagendijk and E. Siegel, Solid State. Commun. 20, 709 (1976).

[6]J. P. Boucher, M. Ahmed-Bakheit, M. Nechtschein, M. Villa, G. Bonera, and F. Borsa, Phys. Rev. B 13, 4098 (1976).

[7]A. Lagendijk and D. Schoemaker, Phys. Rev. B 16, 47 (1977).

[8]G. F. Reiter and J. P. Boucher, Phys. Rev. B 11, 1823 (1975).

[9]H. R. Boesch and F. Waldner, in Ref. 4, p. 642.

[10]W. D. van Amstel and L. J. deJongh, Solid State. Commun. 11, 1423 (1972).

[11]H. Remy and G. Laves, Ber. Dtsch. Chem. Ges. 66, 401 (1933).

[12]Y. Okaya *et al.*, Acta Crystallogr. 10, 800 (1957).

[13]T. Morita, Phys. Rev. B 6, 3385 (1972).